Advanced Composite Materials

ISSN: 0924-3046 (Print) 1568-5519 (Online) Journal homepage: http://www.tandfonline.com/loi/tacm20

Free vibration of thick functionally graded carbon nanotube-reinforced rectangular composite plates based on three-dimensional elasticity theory via differential quadrature method

Mohammad Rahim Nami & Maziar Janghorban

To cite this article: Mohammad Rahim Nami & Maziar Janghorban (2015) Free vibration of thick functionally graded carbon nanotube-reinforced rectangular composite plates based on three-dimensional elasticity theory via differential quadrature method, Advanced Composite Materials, 24:5, 439-450, DOI: 10.1080/09243046.2014.901472

To link to this article: http://dx.doi.org/10.1080/09243046.2014.901472

Published online: 26 Mar 2014.

Advanced Composite Materials, 2015
Vol. 24, No. 5, 439–450, http://dx.doi.org/10.1080/09243046.2014.901472

Free vibration of thick functionally graded carbon nanotube-reinforced rectangular composite plates based on three-dimensional elasticity theory via differential quadrature method

Mohammad Rahim Nami and Maziar Janghorban*

Mechanical Engineering School of Shiraz University, Shiraz, Iran

(*Received 8 September 2013; accepted 4 March 2014*)

In this research, the free vibration of thick functionally graded carbon nanotube-reinforced rectangular composite plates is investigated. For this purpose, the three-dimensional elasticity theory, as an appropriate theory for thick plates, is used. In order to discretize the governing equations, the differential quadrature method (DQM) is adopted to solve the governing equations. In the present work, no approximation is used and the DQM is adopted in all directions. Although this may cause the MATLAB code to be longer but it may eliminate extra frequencies which not really exist. The material properties of functionally graded carbon nanotube-reinforced composite plates are assumed to be graded in the thickness direction, and are estimated through a micromechanical model. Numerical results of the present paper are also compared with the results of both isotropic and orthotropic rectangular plates. Additionally, the influences of different parameters such as boundary conditions on the numerical results are also investigated. It is hoped that this research will lead to more detailed models on rectangular composite plates reinforced by carbon nanotubes.

Keywords: free vibration; three-dimensional elasticity theory; thick functionally graded carbon nanotube-reinforced rectangular composite plates; differential quadrature method

1. Introduction

Because of the exceptional mechanical and physical properties, plates and beams reinforced by one-dimensional nanostructures are widely investigated in the past decade. The load transfer efficiency from surrounding matrix to the carbon nanotubes (CNTs) in the CNTs-reinforced nanocomposites was studied by Tsai and Lu.[1] Both single-walled CNTs (SWCNTs) and multi-walled CNTs (MWCNTs) were taken into account in the investigation. Jafari Mehrabadi et al. [2] studied the mechanical buckling of a functionally graded nanocomposite rectangular plate reinforced by aligned and straight SWCNTs subjected to uniaxial and biaxial in-plane loadings. The equilibrium and stability equations are derived using the Mindlin plate theory considering the first-order shear deformation effect and variational approach. Mosallaie Barzoki et al. [3] analyzed the effect of partially filled polyethylene (PE) foam core on the behavior of torsional buckling of an isotropic, simply supported piezoelectric polymeric cylindrical shell made from polyvinylidene fluoride (PVDF), and subjected to combined electro-thermo-mechanical

*Corresponding author. Email: maziar.janghorban@gmail.com

loads. Wang and Shen [4] presented the nonlinear vibration, nonlinear bending, and post-buckling analyses for a sandwich plate with FGM face sheets resting on an elastic foundation in thermal environments. The material properties of FGM face sheets were assumed to be graded in the thickness direction according to a simple power law distribution. Mosallaie Barzoki et al. [5] investigated the nonlinear buckling response of a composite cylindrical shell made of polyvinylidene fluoride. A two-dimensional smart model surrounded by an elastic foundation subjected to combined electro-thermo-mechanical loading was considered. Rokni et al. [6] obtained a new two-dimensional (2D) optimum distribution of CNTs in the longitudinal and thickness directions of a polymer composite micro-beam to achieve its highest fundamental natural frequency given a weight percent (wt.%) of CNTs. SWNTs dispersed with various solvents were incorporated into epoxy matrix via sonication method by Lau et al.[7] Dynamics differential scanning calorimetry (DSC) results indicated that even small traces of residual solvent in the composite processing had a great impact on the cure reaction and subsequently affected the endothermic behaviors of the nanocomposites. Seidel and Puydupin-Jamin [8] developed a multi-scale model based on computational micromechanics techniques for determining the effective electrical conductivity of carbon nanotube–polymer nanocomposites containing bundles of SWCNTs at a wide range of SWCNT volume fractions above and below the observed percolation concentrations. Salehi-Khojin and Jalili [9] investigated the buckling behavior of BNNT-reinforced piezoelectric polymeric composites when subjected to combined electro-thermo-mechanical loadings. For this, the multi-walled structure of BNNT was considered as elastic media and a set of concentric cylindrical shells with van der Waals interaction between them. Thermal buckling and post-buckling behaviors were presented for functionally graded nanocomposite plates reinforced by SWCNTs subjected to in-plane temperature variation by Shen and Zhang.[10] Ke et al. [11] considered the nonlinear free vibration of functionally graded nanocomposite beams reinforced by SWCNTs based on Timoshenko beam theory and von Kármán geometric nonlinearity.

In this paper, for solving the governing equations, the differential quadrature method is used. The results for free vibration of thick functionally graded carbon nanotube-reinforced rectangular composite plates based on three-dimensional analysis are given for the first time and these can serve as reference values for other analyses.

The remainder of this paper is organized as follows: In Section 2, the material properties of functionally graded carbon nanotube-reinforced rectangular composite plates are presented. In this section, different kinds of functionally graded nanocomposites are shown. Next, in Section 3, the governing equations based on the three-dimensional elasticity theory are derived using the constitutive relations, the strain–displacement relations, and the equilibrium equations. In Section 4, the numerical results are presented and the effects of different parameters are discussed. Finally in Section 5, the whole paper is briefly investigated. The overall view on the differential quadrature method as a numerical tool is also presented in the Appendix A.

2. Material properties

Nanocomposites are the materials filled with nano-sized particles, that is, particles with at least one dimension in the nanometer scale. There are two types of nanoparticles that are used often for this purpose, platelets and nanotubes, although spherical particles are also being considered.[12] In the present work, the functionally graded carbon nanotube-reinforced rectangular composite plates are investigated. The nanotubes are

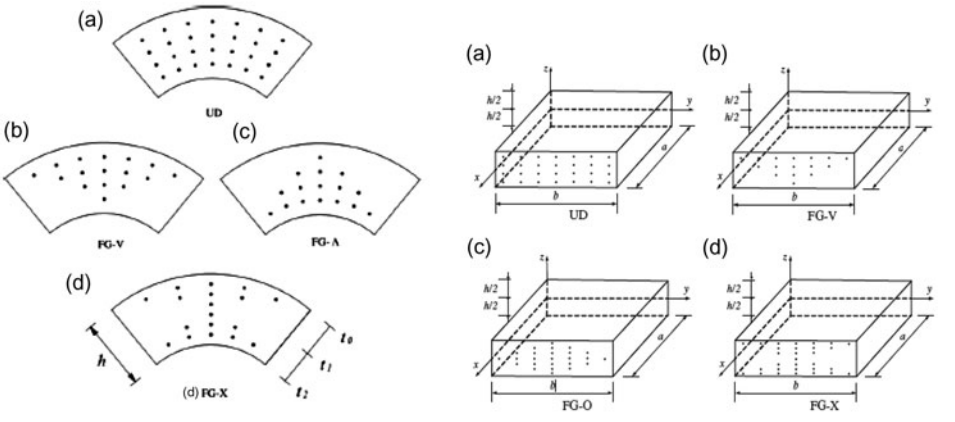

Figure 1. Functionally graded carbon nanotube-reinforced composite plates [13,14].

distributed through the thickness of the plate so the material properties vary according to the z component. The nanotubes are distributed through the thickness of the plate so the material properties are varying through the thickness of functionally graded rectangular nanocomposites. According to the rule of mixture, the effective Young's modulus and shear modulus can be expressed as,[13]

$$E_{11} = \eta_1 V_{\mathrm{CNT}} E_{11}^{\mathrm{CNT}} + E^m V_m \tag{1}$$

$$(\eta_2/E_{22}) = (V_{\mathrm{CNT}}/E_{22}^{\mathrm{CNT}}) + (V_m/E^m) \tag{2}$$

$$(\eta_3/G_{12}) = (V_{\mathrm{CNT}}/G_{12}^{\mathrm{CNT}}) + (V_m/G^m) \tag{3}$$

The density of the composite material can be obtained easily in the terms of the densities of the constituents and their volume fractions.[13]

$$\rho = V_{\mathrm{CNT}} \rho^{\mathrm{CNT}} + \rho^m V_m \tag{4}$$

From the knowledge of authors, there are five types of nanocomposites which are mostly studied in these years, (1) UD CNTRC plate, (2) FG-V CNTRC plate, (3) FG-X CNTRC plate, (4) FG-Λ CNTRC plate, and (5) FG-O CNTRC plate (Figure 1).

3. Governing equations

In many industrial situations, it is crucial to accurately predict the free vibration characteristics of rectangular plates, as the key structural components are used in a wide range of applications from space vehicles to microelectromechanical system (MEMS) devices.[15] For investigating the vibration of thick plates, the three-dimensional elasticity solutions have the ability to express precisely the high-order variation displacement through the thickness of the plate. Although such a three-dimensional approach is rigorous, finding solutions is generally extremely difficult. The few analytical solutions available are usually restricted to problems with simple plate geometry, loading conditions, and boundary conditions.[16] To construct a general three-dimensional constitutive law for the linear

elastic materials, one can assume that each stress component is linearly related to each strain component. These relations can be cast into a matrix format as follows [17]:

$$\begin{Bmatrix} \sigma_{xx} \\ \sigma_{yy} \\ \sigma_{zz} \end{Bmatrix} = \begin{bmatrix} C_{11} & C_{12} & C_{13} \\ C_{12} & C_{22} & C_{23} \\ C_{13} & C_{23} & C_{33} \end{bmatrix} \begin{Bmatrix} \varepsilon_{xx} - \alpha_1 \Delta T \\ \varepsilon_{yy} - \alpha_2 \Delta T \\ \varepsilon_{zz} - \alpha_3 \Delta T \end{Bmatrix} \begin{Bmatrix} \sigma_{yz} \\ \sigma_{xz} \\ \sigma_{xy} \end{Bmatrix} = \begin{Bmatrix} C_{44}\gamma_{yz} \\ C_{55}\gamma_{xz} \\ C_{66}\gamma_{xy} \end{Bmatrix} \tag{5a-f}$$

where σ_{ij} ($i, j = x, y, z$) are the stress tensor components; ε_{ii} and γ_{ij} ($i, j = x, y, z$; $i \neq j$) are the normal and shearing components of the strain tensor, respectively. All stress fields must satisfy the equilibrium equations in order to be in static equilibrium. The equilibrium equations can be defined as follows [17]:

$$\begin{aligned} \partial\sigma_x/\partial x + \partial\tau_{xy}/\partial y + \partial\tau_{zx}/\partial z + F_x = 0 \\ \partial\sigma_y/\partial y + \partial\tau_{xy}/\partial x + \partial\tau_{zy}/\partial z + F_y = 0 \\ \partial\sigma_z/\partial z + \partial\tau_{yz}/\partial y + \partial\tau_{xz}/\partial x + F_z = 0 \end{aligned} \tag{6}$$

Three normal and three shearing strain components leading to a total of six independent components that completely describe small deformation theory are defined. This set of equations is normally referred to as the strain–displacement relations.[17]

$$\begin{aligned} \varepsilon_x = \partial u/\partial x, \varepsilon_y = \partial v/\partial y, \varepsilon_z = \partial w/\partial z \\ \gamma_{xy} = \partial u/\partial y + \partial v/\partial x, \\ \gamma_{xz} = \partial u/\partial z + \partial w/\partial x, \\ \gamma_{yz} = \partial v/\partial z + \partial w/\partial y, \end{aligned} \tag{7}$$

where u, v and w are the displacements in the x, y and z, respectively. In practice, the body forces are usually eliminated and the weight of the plate as surface force $p_z(x, y)$ acting on the lower and upper faces of the plate is applied. A similar approach is taken with the external load acting in the transverse direction.[18] The formulation of the present theory is based on normal technique (using Equation (6), equilibrium equations and Equation (7) strain–displacement relations). By substituting the strain–displacement relations to the three-dimensional constitutive relations, one can find the relations between the stresses and displacements. By substituting these stresses into the equilibrium equations, the governing equations in terms of displacement components for thick functionally graded carbon nanotube-reinforced rectangular composite plates can be written as,

$$\begin{aligned} &C_{11}\frac{\partial^2 u_0}{\partial x^2} + C_{66}\frac{\partial^2 u_0}{\partial y^2} + (C_{12} + C_{66})\frac{\partial^2 v_0}{\partial x \partial y} + C'_{55}\frac{\partial u_0}{\partial z} + C_{55}\frac{\partial^2 u_0}{\partial z^2} + C'_{55}\frac{\partial w_0}{\partial x} \\ &+ (C_{13} + C_{55})\frac{\partial^2 w_0}{\partial x \partial z} = \rho\frac{\partial^2 u_0}{\partial t^2} + (C_{12} + C_{66})\frac{\partial^2 u_0}{\partial x \partial y} + C_{66}\frac{\partial^2 v_0}{\partial x^2} + C_{22}\frac{\partial^2 v_0}{\partial y^2} + C'_{44}\frac{\partial v_0}{\partial z} \\ &+ C_{44}\frac{\partial^2 v_0}{\partial z^2} + C'_{44}\frac{\partial w_0}{\partial y} + (C_{23} + C_{44})\frac{\partial^2 w_0}{\partial y \partial z} = \rho\frac{\partial^2 v_0}{\partial t^2} \end{aligned} \tag{8a, b}$$

$$C'_{13}\frac{\partial u_0}{\partial x}+(C_{13}+C_{55})\frac{\partial^2 u_0}{\partial x\partial z}+C'_{23}\frac{\partial v_0}{\partial y}+(C_{23}+C_{44})\frac{\partial^2 v_0}{\partial y\partial z}+C_{55}\frac{\partial^2 w_0}{\partial x^2}+C_{44}\frac{\partial^2 w_0}{\partial y^2}+C'_{33}\frac{\partial w_0}{\partial z}+C_{33}\frac{\partial^2 w_0}{\partial z^2}=\rho\frac{\partial^2 w_0}{\partial t^2} \tag{9}$$

where $u_0 = u_0\ (x, y, z)$, $v_0 = v_0\ (x, y, z)$, and $w_0 = w_0\ (x, y, z)$ are the displacement components along the x, y and z-axis, respectively. Hereafter, a subscript '0' is used to represent the deformation field variables and the stress components in the equilibrium state.

Equation (5) represents the in-plane equilibrium equations along the x- and y-axis; and Equation (6) is the transverse or the out-of-plane equilibrium equation. Because of the complexity of the above equations, it may be very difficult to solve these equations analytically. So, numerical methods may be useful to discretize the above equations. One of the numerical methods which has been used several times for studying plates is the differential quadrature method. The author knows two major characteristics for this method, (1) fast convergency of this method and (2) accuracy of this method. The differential quadrature method is employed to solve these equations. The equilibrium Equations (5) and (6) can be discretized as Equation (8a, b):

$$C_{11}\sum_{m=1}^{N_x}B^x_{im}u_{0mjk}+C_{66}\sum_{n=1}^{N_y}B^y_{jn}u_{0ink}+(C_{12}+C_{66})\sum_{m=1}^{N_x}\sum_{n=1}^{N_y}A^x_{im}A^y_{jn}v_{0mnk}+C'_{55}\sum_{p=1}^{N_z}A^z_{kp}u_{0i\,jp}+C_{55}\sum_{p=1}^{N_z}B^z_{kp}u_{0i\,jp}+C'_{55}\sum_{m=1}^{N_x}A^x_{im}w_{0mjk}+(C_{13}+C_{55})\sum_{m=1}^{N_x}\sum_{p=1}^{N_z}A^x_{im}A^z_{kp}w_{0mjp}=\rho\omega^2u_{ijk}$$

$$(C_{12}+C_{66})\sum_{m=1}^{N_x}\sum_{n=1}^{N_y}A^x_{im}A^y_{jn}u_{0mnk}+C_{66}\sum_{m=1}^{N_x}B^x_{im}v_{0mjk}+C_{22}\sum_{n=1}^{N_y}B^y_{jn}v_{0ink}+C'_{44}\sum_{p=1}^{N_Z}A^z_{kp}v_{0i\,jp}+C_{44}\sum_{p=1}^{N_z}B^z_{kp}v_{0i\,jp}+C'_{44}\sum_{n=1}^{N_y}A^y_{jn}w_{0ink}+(C_{23}+C_{44})\sum_{n=1}^{N_y}\sum_{p=1}^{N_z}A^y_{jn}A^z_{kp}w_{0inp}=\rho\omega^2v_{ijk} \tag{10a, b}$$

Equation (9):

$$C'_{13}\sum_{m=1}^{N_x}A^x_{im}u_{0mjk}+(C_{13}+C_{15})\sum_{m=1}^{N_x}\sum_{p=1}^{N_z}A^x_{im}A^z_{kp}u_{0mjp}+C'_{23}\sum_{m=1}^{N_x}A^x_{im}v_{0mjk}+(C_{23}+C_{44})\sum_{m=1}^{N_x}\sum_{p=1}^{N_z}A^x_{im}A^z_{kp}v_{0mjp}+C_{55}\sum_{m=1}^{N_x}B^{\xi}_{im}w_{0mjk}+C_{44}\sum_{n=1}^{N_y}B^{\eta}_{jn}w_{0ink}+C'_{33}\sum_{p=1}^{N_z}A^z_{kp}w_{0ijp}+C_{33}\sum_{p=1}^{N_z}B^z_{kp}w_{0ijp}=\rho\omega^2w_{ijk} \tag{11}$$

4. Numerical results

The computer package MATLAB is used to code the expressions obtained by using differential quadrature method, to calculate the natural frequencies for thick/very thick functionally graded carbon nanotube-reinforced rectangular composite plates. The

comparison studies are carried out in order to verify the accuracy and efficiency of the present three-dimensional elasticity theory. Firstly, the convergency of the present method is investigated in Table 1. One can easily find that even six grid points are enough to reach accurate numerical solutions. It is one the advantages of differential quadrature method which may be seen in the most of the works. From this table, one can find that this fast convergency can be achieved for all modes of vibration. Secondly, the results for simply supported rectangular thick plate are compared with the results of Batra et al.[19] From this table, it may be found that the present formulation and MATLAB code written are done properly and this methodology can be used as bench mark for future works. In this comparison, the exact solution for fundamental frequency is also tabulated and our numerical result is in a good agreement with exact solution. As another example, the results of the present work are compared with the results of Matsunaga [20] for thicker square plate. It is good to mention that Matsunaga [20] used 2-D higher-order deformation theory and Batra et al. [19] used higher-order shear and normal deformable plate theory. The result for very thick plate $a/h = 1$ is also verified with the result of ANSYS. It is good to mention that few of formulations can predict the natural frequencies of very thick plates but as one can see in Table 2, present methodology can be used for very thick plates too. From the knowledge of authors, very thick functionally graded nanocomposites have not been studied with any theory yet and it is one the benefits of the present paper. It should be noted that in the review of the literature,[21–27] one may see that some theories give extra frequencies and some of them did not have some frequencies. It may be because of the approximation they used. For example, they assumed sinusoidal displacements in some directions

Table 1. The convergency of the present method for thick carbon nanotube-reinforced rectangular composite plate.

	N_z					
Mode	6	7	8	9	10	11
1	0.6494	0.6494	0.6494	0.6494	0.6494	0.6494
2	0.9742	0.9742	0.9742	0.9742	0.9742	0.9742
3	1.1708	1.1708	1.1708	1.1708	1.1708	1.1708
4	1.2995	1.2995	1.2995	1.2995	1.2995	1.2995
5	1.4492	1.3963	1.4572	1.4173	1.4591	1.4278
6	1.6241	1.6241	1.6241	1.6241	1.6241	1.6241
7	1.7863	1.7566	1.7936	1.7706	1.7954	1.7773
8	1.8872	1.8872	1.8872	1.8872	1.8872	1.8872
9	1.9492	1.9492	1.9492	1.9492	1.9492	1.9492
10	2.0545	2.0545	2.0537	2.0537	2.0537	2.0537

Table 2. Comparison of the nondimensional natural frequency parameters of simply supported thick isotropic plate.

Thick plates					Very thick plates	
$a/b = 2, a/h = 4$			$a/b = 1, a/h = 2$		$a/b = 1, a/h = 1$	
Present	Batra [19]	Exact[a]	Present	Matsunaga [20]	Present	ANSYS
0.7854	0.7854	0.7857	0.9742	0.9400	1.9483	1.9492

[a]Exact solutions are also listed in Batra [19].

and then solve the remaining problem. Another reason for reaching extra frequencies may be because of using wrong theories such as using first-order shear deformation theory for thick plates. In the present work, no approximation is used and the differential quadrature method is adopted in all directions and an appropriate theory is used for studying thick plates. The authors suggest the researchers to investigate more about the extra frequencies which not really exist. In Table 3 the material properties for functionally graded carbon nanotube-reinforced rectangular composite plates are tabulated. The results are also verified with the results of molecular dynamics simulations of polymer/carbon nanotube composites done by Han and Elliott.[28] One can see good agreement between the results for different V^*_{CNT} which is defined as follows [29]:

$$V^*_{\mathrm{CNT}} = W_{\mathrm{CNT}}/(W_{\mathrm{CNT}} + (\rho_{\mathrm{CNT}}/\rho_m) - (\rho_{\mathrm{CNT}}/\rho_m)W_{\mathrm{CNT}}) \tag{12}$$

For the material properties of CNTs, different reports are available. In Table 4, the temperature-dependent properties for armchair (10,10) single-walled carbon nanotube are presented.[13,29,30]

It seems that most of the works because of the approximation of harmonic motion in one or two directions cannot investigate the fully clamped structures. So, it may be useful to study fully clamped plates in this work. In Table 5, the results for fully

Table 3. Material properties of functionally graded carbon nanotubes-reinforced rectangular composite plates for different V^*_{CNT}.

V^*_{CNT}	E_{11}(GPa)	E_{11}(GPa) [28]	E_{22}(GPa)	E_{22}(GPa) [28]
0.11	94.42	94.8	2.204	2.2
0.14	120.4	120.2	2.298	2.3
0.17	144.8	145.6	3.494	3.5

Table 4. Temperature-dependent material properties of (10, 10) single-walled carbon nanotube.

Temperature (K)	E_{11}^{CNT}	E_{22}^{CNT}	G_{12}^{CNT}
300	5.6466	7.0800	1.9445
500	5.5308	6.9348	1.9643
700	5.4744	6.8641	1.9644

Table 5. The effects of V^*_{CNT} on the natural frequencies of fully clamped rectangular composite plates with uniformly distributed carbon nanotubes.

Mode	$V^*_{\mathrm{CNT}} = .11$	$V^*_{\mathrm{CNT}} = .14$	$V^*_{\mathrm{CNT}} = .17$
1	1.9342	1.95	2.19
2	2.1847	2.22	2.73
3	3.0362	3.04	3.2
4	3.0803	3.12	3.71
5	3.2331	3.29	3.77
6	3.404	3.42	4.04
7	3.6531	3.72	4.38
8	3.7935	3.85	4.38
9	3.8685	3.90	4.57
10	4.1576	4.20	4.64

clamped rectangular composite plates with uniformly distributed CNTs are presented. The first 10 frequencies of fully clamped rectangular composite plates are presented. The effect of V^*_{CNT} is also investigated on the natural frequencies of nanocomposites in this table. It is shown that increasing the V^*_{CNT} will increase the natural frequencies. From this table, it is seen that the natural frequencies for $V^*_{CNT} = 0.11$ and $V^*_{CNT} = 0.14$ can be assumed same but the results of $V^*_{CNT} = 0.17$ are different. This conclusion may be extended to almost all the modes of vibration.

In Table 6, the first 10 frequencies of thick functionally graded carbon nanotube-reinforced rectangular composite plates are tabulated. It is assumed that the CNTs are arranged as Figure 1, known as FG-O. It is also assumed that the plate is clamped-simply supported (CSCS) case. It is shown that increasing the V^*_{CNT} will lead to increase the natural frequencies of functionally graded carbon nanotube-reinforced rectangular composite plates with FG-O arrangement. By comparing the results presented in Tables 5 and 6, it is found that the natural frequencies tabulated in Table 5 have higher values

Table 6. The effects of V^*_{CNT} on the natural frequencies of CSCS rectangular functionally graded nanocomposites (FG-O).

Mode	$V^*_{CNT} = .11$	$V^*_{CNT} = .14$	$V^*_{CNT} = .17$
1	1.3843	1.4104	1.7366
2	1.9351	1.9512	2.1956
3	2.1656	2.2038	2.7072
4	2.7680	2.8198	3.2093
5	3.0410	3.0465	3.4710
6	3.0834	3.1294	3.7032
7	3.1522	3.2282	3.7267
8	3.2298	3.2892	3.9951
9	3.3739	3.3863	4.0418
10	3.6534	3.7089	4.3916

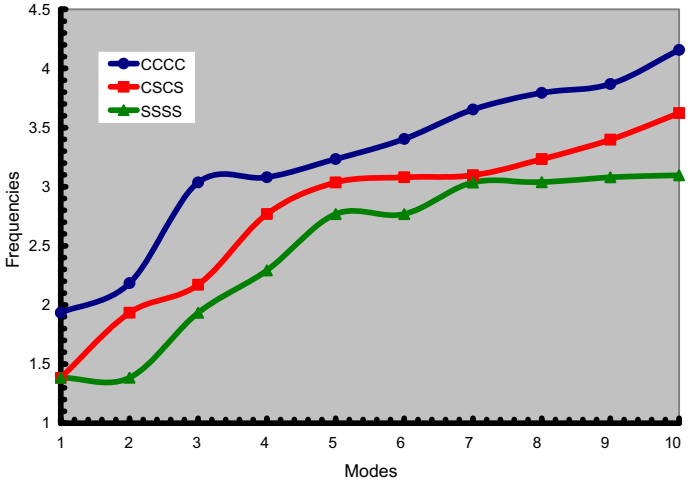

Figure 2. The influences of different boundary conditions on the natural frequencies of functionally graded carbon nanotube-reinforced rectangular composite plates.

Table 7. Natural frequencies of simply supported rectangular functionally graded nanocomposite plates with $V^*_{CNT} = 0.14$.

Mode	UD	FG-X	FG-O
1	1.4088	1.4174	1.4089
2	1.4088	1.4188	1.4104
3	1.9490	1.9584	1.9539
4	2.3345	2.3854	2.3175
5	2.8176	2.8335	2.8167
6	2.8176	2.8364	2.8198
7	3.0399	3.0445	3.0411
8	3.0420	3.0487	3.0465
9	3.1230	3.1079	3.1358
10	3.1523	3.1341	3.2282

in comparison with the results in Table 6. This conclusion is correct for first 10 frequencies and all the values of V^*_{CNT}.

In Figure 2, the influences of different boundary conditions on the free vibration of functionally graded carbon nanotube-reinforced rectangular composite plates are investigated. It is found that the natural frequencies are increasing as follows,

$$\text{CCCC} > \text{CSCS} > \text{SSSS}$$

It is mentioned that CCCC and SSSS are referred to as fully clamped and simply supported boundary conditions and CSCS is referred to as clamped-simply supported boundary condition. This figure shows us the influence of boundary condition on natural frequencies can be ignored in some modes of vibration but it cannot be extended to all modes of vibration.

In Table 7, the effects of different arrangements of CNTs-reinforced nanocomposite plates are tabulated. Three kinds of functionally graded nanocomposites are investigated,

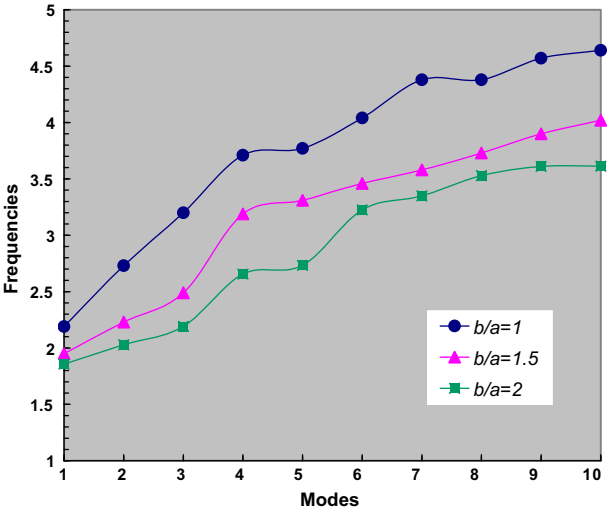

Figure 3. The influences of aspect ratio on the natural frequencies of thick uniformly distributed carbon nanotube-reinforced rectangular composite plates.

(1) UD, (2) FG-X, and (3) FG-O. In this table, simply supported rectangular nanocomposites are studied. It is shown that the natural frequencies behave usually as follows,

$$\mathrm{FG}-\mathrm{X} > \mathrm{FG}-\mathrm{O} > \mathrm{UD}$$

As another example, in Figure 3, the influences of aspect ratio on the natural frequencies of thick uniformly distributed carbon nanotube-reinforced rectangular composite plates are shown. The boundary condition of the nanocomposites is assumed to be fully clamped. It is also assumed that V^*_{CNT} is 0.17. As it may be expected, one can easily found that with the increase of aspect ratio, the natural frequencies will decrease.

5. Conclusion

Derived herein were the governing equations for the free vibration analysis of functionally graded carbon nanotube-reinforced rectangular composite plates based on the three-dimensional elasticity theory. In order to solve the equations of motion, the differential quadrature was used. The present results were compared with the results of simply supported isotropic and orthotropic plates. Good agreement was achieved in this paper. In the present paper, three kinds of functionally graded nanocomposites were investigated, (1) UD (2) FG-X (3) FG-O.

In this work,

(1) It was obtained that increasing the V^*_{CNT} will increase the natural frequencies of fully clamped rectangular composite plates with uniformly distributed CNTs.
(2) It was found that the natural frequencies are increasing as follows,

$$\mathrm{CCCC} > \mathrm{CSCS} > \mathrm{SSSS}$$

(3) It was shown that the natural frequencies behave usually as follows

$$\mathrm{FG}-\mathrm{X} > \mathrm{FG}-\mathrm{O} > \mathrm{UD}$$

(4) It was obtained that with the increase of aspect ratio, the natural frequencies will decrease for fully clamped rectangular composite plates with uniformly distributed CNTs.

References

[1] Tsai JL, Lu TC. Investigating the load transfer efficiency in carbon nanotubes reinforced nanocomposites. Compos Struct. 2009;90:172–179.
[2] Mehrabadi SJ, Aragh BS, Khoshkhahesh V, Taherpour A. Mechanical buckling of nanocomposite rectangular plate reinforced by aligned and straight single-walled carbon nanotubes. Compos. Part B. 2012;43:2031–2040.
[3] Mosallaie Barzoki AA, Ghorbanpour Arani A, Kolahchi R, Mozdianfard MR. Electro-thermo-mechanical torsional buckling of a piezoelectric polymeric cylindrical shell reinforced by DWBNNTs with an elastic core. Appl. Math. Model. 2011;36:2983–2995.
[4] Wang Z-X, Shen H-S. Nonlinear analysis of sandwich plates with FGM face sheets resting on elastic foundations. Compos. Struct. 2011;93:2521–2532.
[5] Mosallaie Barzoki AA, Ghorbanpour Arani A, Kolahchi R, Mozdianfard MR, Loghman A. Nonlinear buckling response of embedded piezoelectric cylindrical shell reinforced with BNNT under electro–thermo-mechanical loadings using HDQM. Compos. Part B. 2012;2012:722–727.

[6] Rokni H, Milani AS, Seethaler RJ. 2D optimum distribution of carbon nanotubes to maximize fundamental natural frequency of polymer composite micro-beams. Compos. Part B. 2012;43:779–785.
[7] Lau KT, Lu M, Cheung H, Sheng F, Li H, Li HL. Thermal and mechanical properties of single-walled carbon nanotube bundle-reinforced epoxy nanocomposites: the role of solvent for nanotube dispersion. Compos. Sci. Technol. 2005;65:719–725.
[8] Seidel GD, Puydupin-Jamin AS. Analysis of clustering, interphase region, and orientation effects on the electrical conductivity of carbon nanotube–polymer nanocomposites via computational micromechanics. Mech. Mater. 2011;43:755–774.
[9] Salehi-Khojin A, Jalili N. Buckling of boron nitride nanotube reinforced piezoelectric polymeric composites subject to combined electro-thermo-mechanical loadings. Compos. Sci. Technol. 2008;68:1489–1501.
[10] Shen HS, Zhang CL. Thermal buckling and postbuckling behavior of functionally graded carbon nanotube-reinforced composite plates. Mater. Des. 2010;31:3403–3411.
[11] Ke LL, Yang J, Kitipornchai S. Nonlinear free vibration of functionally graded carbon nanotube-reinforced composite beams. Compos. Struct. 2010;92:676–683.
[12] Agarwal B, Lawrence D, Broutman J, Chandrashekhara K. Analysis and performance of fiber composites. Hoboken (NJ): Wiley; 2006.
[13] Zhu P, Lei ZX, Liew KM. Static and free vibration analyses of carbon nanotube-reinforced composite plates using finite element method with first order shear deformation plate theory. Compos. Struct. 2012;94:1450–1460.
[14] Shen HS, Xiang Y. Nonlinear vibration of nanotube-reinforced composite cylindrical shells in thermal environments. Comput. Meth. Appl. Mech. Eng. 2012;213–216:196–205.
[15] Hosseini-Hashemi S, Fadaee M, Rokni Damavandi Taher H. Exact solutions for free flexural vibration of Lévy-type rectangular thick plates via third-order shear deformation plate theory. Appl. Math. model. 2011;35:708–727.
[16] Szilard R. Theories and applications of plate analysis: Classical, numerical and engineering methods. Hoboken (NJ): Wiley; 2004.
[17] Sadd MH. Elasticity, theory, applications, and numerics. Burlington (MA): Elsevier; 2009.
[18] Srinivas S, Joga Rao CV, Rao AK. An exact analysis for vibration of simply-supported homogeneous and laminated thick rectangular plates. J. Sound Vib. 1970;12:187–199.
[19] Batra RC, Immaee SA. Vibrations of thick isotropic plates with higher order shear and normal deformable plate theories. Comput. Struct. 2007;78:433–439.
[20] Matsunaga H. Free vibration and stability of functionally graded plates according to a 2-D higher-order deformation theory. Compos. Struct. 2008;82:499–512.
[21] Batra RC, Qian LF, Chen LM. Natural frequencies of thick square plates made of orthotropic, trigonal, monoclinic, hexagonal and triclinic materials. J. Sound Vib. 2004;270:1074–1086.
[22] Batra RC, Aimmanee S. Missing frequencies in previous exact solutions of free vibrations of simply supported rectangular plates. J. Sound Vib. 2003;265:887–896.
[23] Ferreira AJM, Batra RC. Natural frequencies of orthotropic, monoclinic and hexagonal plates by a meshless method. J Sound Vib. 2005;285:734–742.
[24] Ferreira AJM, Fasshauer GE, Batra RC. Natural frequencies of thick plates made of orthotropic, monoclinic, and hexagonal materials by a meshless method. J. Sound Vib. 2009;319:984–992.
[25] Chao CC, Chern YC. Comparison of natural frequencies of laminates by 3-D theory, part I: Rectangular plates. J. Sound Vib. 2000;230:985–1007.
[26] Reddy JN. Free vibration of anisotropic, angle-ply laminated plates including transverse shear deformation by the finite element method. J. Sound Vib. 1979;66:565–576.
[27] Huang KH, Dasgupta A. A layer-wise analysis for free vibration of thick composite cylindrical shells. J. Sound Vib. 1995;186:207–222.
[28] Han Y, Elliott J. Molecular dynamics simulations of the elastic properties of polymer/carbon nanotube composites. Comput. Mat. Sci. 2007;39:315–323.
[29] Shen HS. Nonlinear bending of functionally graded carbon nanotube-reinforced composite plates in thermal environments. Compos. Struct. 2009;91:9–19.
[30] Shen HS, Zhang CL. Thermal buckling and postbuckling behavior of functionally graded carbon nanotube-reinforced composite plates. Mater. Des. 2010;31:3403–3411.

[31] Civalek Ö. Application of differential quadrature (DQ) and harmonic differential quadrature (HDQ) For buckling analysis of thin isotropic plates and elastic columns. Eng Struct. 1999;26:171–186.
[32] Liew KM, Teo TM, Han JB. Comparative accuracy of DQ and HDQ methods for three-dimensional vibration analysis of rectangular plates. Int. J. Numer. Meth. Eng. 1999;45:1831–1848.
[33] Liew KM, Teo TM. Modeling via differential quadrature method: three-dimensional solutions for rectangular plates. Comput. Methods Appl. Mech. Eng. 1999;159:369–381.
[34] Liew KM, Teo TM. Three-dimensional vibration analysis of rectangular plates based on differential quadrature method. J. Sound Vib. 1999;220:577–599.
[35] Xu QW, Li ZF, Wang J, Mao JF. Modeling of transmission lines by the differential quadrature method. IEEE Microw. Guided W. 1999;9:145–147.
[36] Xu QW, Mazumder P. Accurate modeling of lossy nonuniform transmission lines by using differential quadrature methods. IEEE Trans. Microw, Theory. 2002;50:2233–2246.
[37] Malekzadeh P. A differential quadrature nonlinear free vibration analysis of laminated composite skew thin plates. Thin-Walled Struct. 2007;45:237–250.
[38] Malekzadeh P, Karami G. A mixed differential quadrature and finite element free vibration and buckling analysis of thick beams on two-parameter elastic foundations. Appl. Math. Model. 2008;32:1381–1394.
[39] Hashemi MR, Abedini MJ, Malekzadeh P. A differential quadrature analysis of unsteady open channel flow. Appl. Math. Model. 2007;31:1594–1608.
[40] Hashemi MR, Abedini MJ, Malekzadeh P. Numerical modeling of long waves in shallow water using incremental differential quadrature method. Ocean Eng. 2006;33:1749–1764.

Appendix A. DQ weighting coefficients

The differential quadrature method (DQM) has attracted appreciable attention over the past two decades.[31–40] In this paper, this interesting (numerical) technique is used which is a fundamental analytical technique. The initial idea dates back to the work of Bellman and Casti. The idea of the differential quadrature method is to quickly compute the derivative of a function at any grid point within its bounded domain by estimating a weighted linear sum of values of the function at a small set of points related to the domain.

In order to illustrate the DQ approximation, consider a function $f(\xi, \eta)$ having its field on a rectangular domain $0 \le \xi \le a$ and $0 \le \eta \le b$ let, in the given domain, the function values be known or desired on a grid of sampling points. According to DQ method, the rth derivative of a function $f(\xi, \eta)$ can be approximated as

$$\left.\frac{\partial^r f(\xi,\eta)}{\partial \xi^r}\right|_{(\xi,\eta)=(\xi_i,\eta_j)} = \sum_{m=1}^{N_\xi} A_{im}^{\xi(r)} f(\xi_m,\eta_j) = \sum_{m=1}^{N_\xi} A_{im}^{\xi(r)} f_{mj} \tag{A.1}$$

for $i = 1, 2, \ldots, N_\xi, j = 1, 2, \ldots, N_\eta$ and $r = 1, 2, \ldots, N_\xi - 1$

From this equation one can deduce that the important components of DQ approximations are weighting coefficients and the choice of sampling points. In order to determine the weighting coefficients, a set of test functions should be used in Equation (A.1). For polynomial basis functions DQ, a set of Lagrange polynomials are employed as the test functions. The weighting coefficients for the first-order derivatives in ξ-direction are thus determined as

$$A_{ij}^{\xi} = \begin{cases} \frac{1}{L_\xi}\frac{M(\xi_i)}{(\xi_i-\xi_j)M(\xi_j)} & \text{for} \quad i \neq j \quad i,j = 1,2,\ldots,N_\xi \\ -\sum\limits_{j=1 i\neq j}^{N_\xi} A_{ij}^{\xi} & \text{for} \quad i \neq j; \end{cases} \tag{A.2}$$

where L_ξ is the length of domain along the ξ - direction and $M(\xi_i) = \prod_{k=1, i\neq k}^{N_\xi} (\xi_i - \xi_k)$

The weighting coefficients of second-order derivative can be obtained as,

$$[B_{ij}^{\xi}] = [A_{ij}^{\xi}][A_{ij}^{\xi}] = [A_{ij}^{\xi}]^2 \tag{A.3}$$

In a similar manner, the weighting coefficients for η-direction can be obtained.